Heliyon 9 (2023) e12871

Contents lists available at ScienceDirect

Heliyon

journal homepage: www.cell.com/heliyon

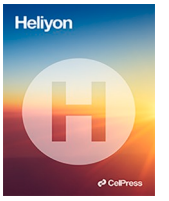

Research article

Mechanical property of pixel extrusion and pin forming for polymer, ceramic, and metal formation

Kittikhun Khotmungkhun [a,b], Rat Prathumwan [b], Arkorn Chotiyasilp [b], Bhadpiroon Watcharasresomroeng [c], Kittitat Subannajui [b,*]

[a] Faculty of Science and Technology, Rajamangala University of Technology Suvarnabhumi, Nonthaburi, 11000, Thailand
[b] School of Materials Science and Innovation, Material Science and Engineering Program, Faculty of Science, Mahidol University, Bangkok, 10400, Thailand
[c] Faculty of Engineer and Technology, Rajamangala University of Technology Suvarnabhumi, Nonthaburi, 11000, Thailand

ARTICLE INFO

Keywords:
Material forming
3D printing
3D molding

ABSTRACT

The rapid material fabrications in pixel shape were mechanically studied in comparison with FDM and STL 3D printing technique. The pixel extrusion technique was the extrusion with a set of holes in the die. By controlling the flow of each hole in the die, the shape could be adjustable. The pixel molding technique composed of a set of pins. By adjusting the length of pin inside the mold, the shape of cavity could be designed. Compared to 3D printing which requires the material deposition with 2D scanning for several layers, 3D material fabrication by pixel extrusion and pixel molding were much faster; however, their resolutions were still much worse compared to 3D printing at the moment. SEM, Tensile test, flexural test, including hardness were used to observe the properties of pixel extrusion and pixel molding. The pixel molding technique was also used to fabricate many materials to compare the properties such as cement, iron, and silica. Apparently, materials could be formed and mechanical properties were investigated.

1. Introduction

In the modern manufacturing, various production methods of materials and devices are invented for the best fabrication efficiency. Depending on the type of material and application, the fabrication technology might be different. In metal production, there are many choices of fabrication process such as casting, rolling, bending, forging, deep drawing, CNC machining, die casting, sintering and so on. Sintering and casting are also the common processes in ceramic productions. In polymer industry, there are also many production processes such as casting, extrusion, two roll milling, pressing, blow molding, injection molding. Most of industrial production usually requires a considerable investment. For example, if only a few samples are fabricated instead of large-scale production, the production cost per unit could be very high due to expense for die or mold production including the laboring fee. Therefore, most of materials and devices which are regularly used in daily life are mass-produced to achieve an economical cost per unit. However, a small-number fabrication of material and device is now possible with the advent of 3D printing techniques. 3D printing techniques, or rapid prototyping technique, are the techniques to form 3D objects without using permanent mold or die which provide a possibility for a small-scale fabrication of various materials with less monetary investment. It could be used to fabricated various kind of materials such as polymer, ceramics, metal, and semiconductor [1,2]. 3D printing technique could be categorized in many subtypes such as selective

* Corresponding author.
E-mail address: kittitat.sub@mahidol.ac.th (K. Subannajui).

https://doi.org/10.1016/j.heliyon.2023.e12871
Received 15 December 2022; Received in revised form 21 December 2022; Accepted 5 January 2023
Available online 11 January 2023

laser sintering [3], stereolithography [4], fused deposition modelling [5], gel printing [6], multi-microdroplet printing [7] and so on. Each of techniques could print different materials for different purposes [8]. The only drawback for using 3D printing compared to conventional production process in the industry is the production time. Due to laborious movement in 3-dimension, 3D printing becomes a most time-consuming production process [9].

Many research groups and companies are extensively trying to develop fast and efficient methods for the high-speed 3D printing. [10]; [11–13, 32]; In FDM, although most of the printing conditions have been already optimized from the 3D printing company, the printing speed can still be improved by adjusting various conditions such as the filament melting speed, the filament feeding speed, and cartesian-robot scanning speed [14]. For Stereolithography, the printing speed can be improved by increasing the scanning speed, increasing the light intensity, including modifying the chemical components in the 3D printing resin such as initiator, monomer, or oligomer to obtain a faster polymerization speed [15,16]. Nevertheless, the scanning time is still much longer than the fabrication speed in extruder, die casting, blow molding, or most of other processes in the industrial scale productions. In order to overcome the time-consuming problem of conventional 3D printing, the shape designable concept and mass production concept have to be combined [17,18]. In this work, the concepts of die and mold which could shift the shape were demonstrated with comparison between techniques and materials. The material shape could be freely changed according to each pixel in the die and mold. Although the size of each pixel was still big, the pixel size could be drastically decreased just like the size of LED in the past compared to current LED.

2. Experiment setup

The poly lactic acid (PLA) was extruded through the extruder to obtain the FDM filament for 3D printing. The filament was printed through the nozzle with different temperature to observe the effect of printing temperature and mechanical property. The next sample was acrylic sample which was printed by the stereolithography technique from the FormLab 3D printer. PLA was also used to form the sample by using the extruder which can regulate the extrusion channel. Each channel is called pixel. There are valves to open and close the channel for each pixel to control the final shape of the sample. Each pixel has the size of 1×1 cm. The last technique to form material in this work is the polymer casting in which the mold has the metallic pins all over the places. Each metallic pin has the dimension of 1×1 cm and can move in and out freely from one another. The shape in the mold was adjusted and polymer was injected into the mold.

3. Results and discussion

3.1. Comparison between FDM, SLA, PEX, PM techniques

The concept of FDM 3D printing was to melt polymeric filament and to move the nozzle including to deposit the polymer on the substrate at the same time as shown in Fig. 1A. Polymer melted due to the heat from the heating element inside the nozzle, and, at the same time, the step motor fed the filament forward with a programable speed. The nozzle was moved according to the movement of cartesian robot which accurately scanned along the planar of the X–Y axis. The deposition was ongoing until the first layer was completed and the nozzle moved up to the second layer. The scanning started again until the second layer was accomplished. This scanning kept on for many layers until a 3D object with desired shape was obtained. For stereolithography technique in Fig. 1B, a laser was used to activate the polymerization of the monomer/oligomer resin. The laser needed to have enough energy to excite free radical

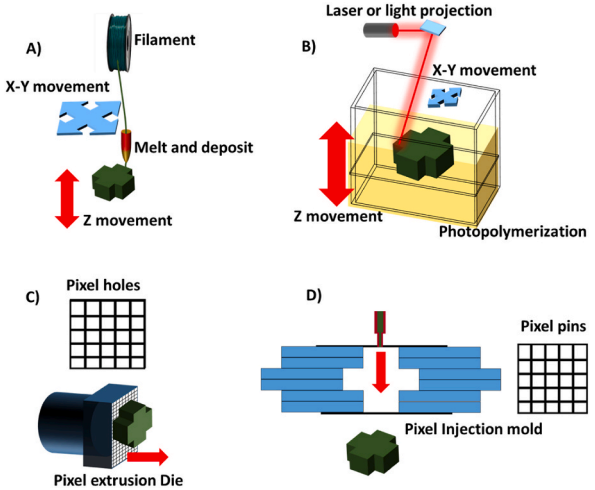

Fig. 1. Shape adjustable rapid prototyping process. (A) FDM 3D printing using polymer filament and cartesian robot (B) Stereolithography using the scanning laser beam on the photopolymer (C) Pixel extrusion with adjustable extruded holes, and (D) injection of various material with adjustable pin.

from photo initiator while moving along X and Y axis. Once the laser scanning of the first layer was completed, the same process was repeated until 3D object was obtained. The scanning speed could be control by mechanical movement of the mirror which directed the beam onto the resin surface. The quality of stereolithography depended on many factors. If the scanning was too fast and absorbed energy was not sufficient to complete the polymerization, the 3D printing quality might be unrefined [19,20]. Furthermore, the scanning speed relied on the mechanical movement of reflective mirror as well [21]. The scanning of cartesian robot in FDM and the scanning of laser in stereolithography played a crucial role in the fabrication speed of 3D printing [15,20].

In Fig. 1C, another 3D shape shifting fabrication method was demonstrated. The extrusion die composed of multi-hole, so called here extrusion pixel, which could freely allow polymer to pass or to stop. By adjusting the valve on each hole, the pixel extrusion (PEX) was obtained. PEX was eligible to extruded long or short samples, and capable of shifting the shape of the sample by turning on and off each pixel. The same concept was also applied to the pixel molding. By dividing the mold wall into many pieces of pixel, the shape of the internal cavity could be designed accordingly. After the polymer was injected inside the mold, the sample was obtained with the same shape as the designed mold. This pin forming or pixel molding (PM) and pixel extrusion (PEX) do not require a long scanning time. As long as the pixel could be controlled separately, the 3D shape could be modified for each production or mass-production. In this experiment, we proved the concept with 3 × 3 pixel PEX and 4 × 4 pixel PIN. The PEX with only one pixel was shown in Fig. 2A, the exact length of extruded material was difficult to controlled since the usual process of extrusion was continuous. The residual internal pressure kept pushing PLA out of the die even after the extrusion process had already stopped. The samples of PEX with 3,6,9 pixels had shown in Fig. 2B, C, 2D respectively. Although, the 3D shape could be successfully modified, the control over the shape and the length were not fully accurate. The samples from PM were shown in Fig. 2E and F. The precision and accuracy of PM was higher than PEX. The PEX was suitable for continuous production as a profile shape sample, and PM was suitable for the stand-alone sample. Unlike typical 3D printing such as FDM or stereolithography, both PEX and PM did not need X–Y axis scanning and the production duration were identical to extrusion and injection molding process; therefore, the production processes were much faster than conventional 3D printing. For a better resolution of sample, smaller pixels and a greater number of pixels could be implemented if this technology was realized and invested. Compared to light emitting diode, the LED 80 years ago was rather big compared to the size of current LED which was commercialized nowadays [22,23].

In Fig. 3A, scanning electron microscope revealed the microstructure of FDM sample which composed of PLA deposition line with the size of 300 μm. This size was identical to the nozzle hole of FDM 3D printer because the deposited material from each layer in FDM process was extruded from a metallic die which had sufficient temperature to melt PLA. The crack observed along the deposition line was the result from rapid cooling of the PLA. In Fig. 3B, the array of scanning had the size of 25–50 μm which was the resolution of each scanning of stereolithography. The material from stereolithography was acrylic with photo initiator, an additive in monomer/oligomer that required a stimulation from photon in laser to start a free radical in polymerization process [15]. The precision of stereolithography was the best compared to other techniques in this paper. The PEX surface morphology was shown in Fig. 3C. The surface of extruded sample was microscopically flat. On the other hand, the surface of PM in Fig. 3D had micro defects which could be the result from the shrinkage during the solidification process inside the mold [24]. The shrinkage was a phenomenon that could commonly occur in the conventional injection molding as well [25,26].

The mechanical properties of FDM, SLA, PEX, and PM samples were shown in Fig. 4. In Fig. 4A, the tensile tests of FDM samples produced from different nozzle temperatures were shown. The tensile forces were aligned with the printed line which were horizontal to the printed layer. The obtained tensile strengths of FDM samples with different nozzle temperatures were not obviously different, but the elongation at break of FDM samples was highest when the nozzle temperature was lowest at 190 °C. This result also implied

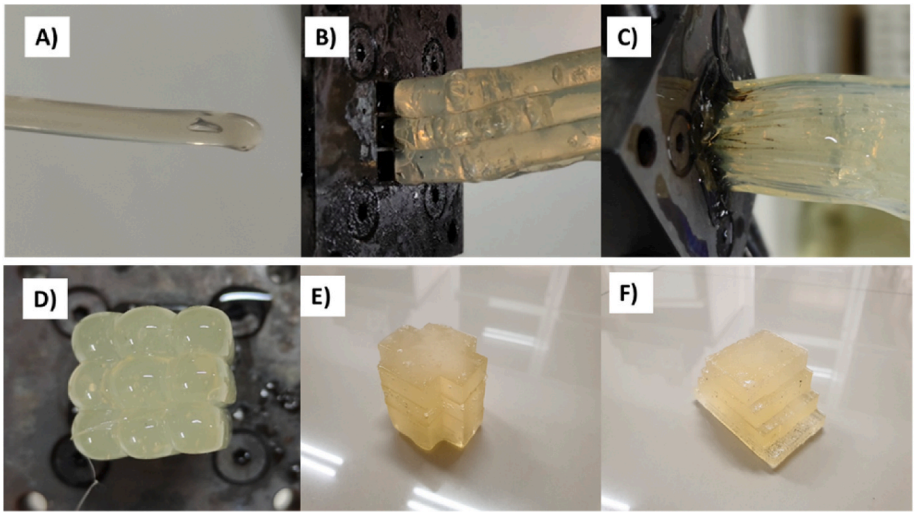

Fig. 2. Pixel extrusion process with (A) 1 channel (B) 3 channels (C) 6 channels (D) 9 channels (E) Pixel molding in cross shape and (F) Pixel molding in pyramid shape.

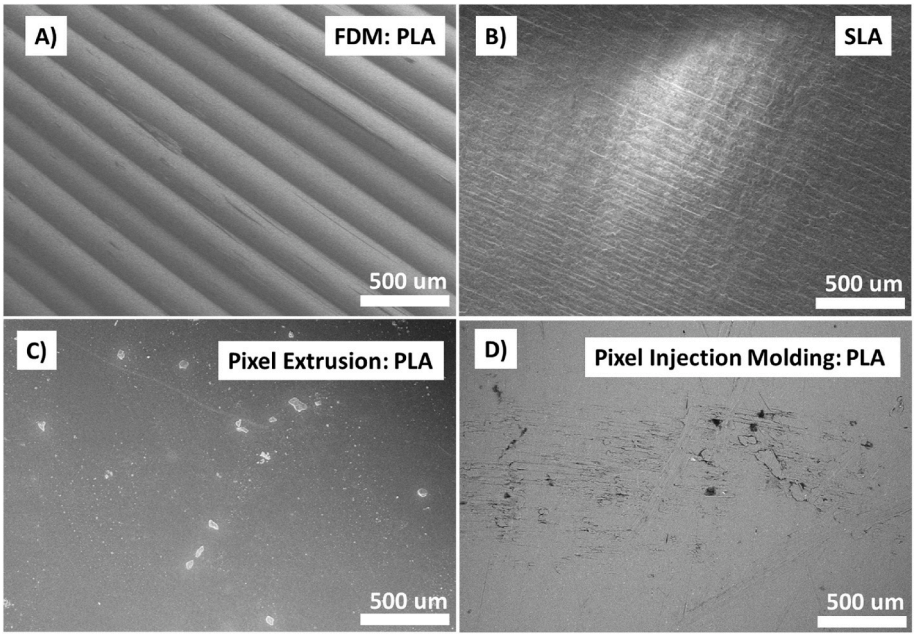

Fig. 3. Surface morphology of (A) FDM sample (B) Stereolithography sample (C) Pixel Extrusion sample (PEX) and (D) Pixel Molding sample (PM sample).

that the toughness of the sample with low deposition temperature was much higher since the area under the stress-strain curve was much larger. Lower toughness at high printed temperature was the effect from the thermal degradation which caused the brittleness of PLA when polymer chains were broken [27,28]. The tensile tests of PLA samples in which the tensile forces were vertical to the printed layer were shown in Fig. 4B. Apparently the tensile strengths had dropped from 60 MPa to below 30 MPa when the tests were performed in the opposite direction to the printed layer. The vertical elongation of FDM samples were also reduced when printed at higher temperature. Conclusively, the mechanical property of FDM sample was anisotropic and depended mainly on the scanning configuration during the printing process. The tensile strength of SLA was 34 MPa with a very low elongation at break of 0.03%. The SLA mechanical test result was inferior to the horizontal test result of FDM samples (PLA) at 190 °C which was stronger and tougher. On the other hand, the SLA process did not require the melting process of polymer; therefore, it did not have temperature variance. Furthermore, the tensile strength was homogeneous compared with FDM samples. The tensile tests of PEX with different temperatures were shown in Fig. 4C. PLA was degraded when processed with higher temperature. Even though the tensile strength was the same at different temperatures, the elongation at breaks was decreased when extruded temperatures were higher. This effect was the same when PLA was processed with PM as shown in Fig. 4D; however, in PM, both tensile strength and elongation at break was reduced when process temperature was higher. The toughness of PM samples was increased when the injection temperature was low to prevent polymer chain degradation [29,30].

In Fig. 4E, the flexural strengths of the FDM samples were tested horizontally. The strengths of samples which passed high temperature process were slightly lower but the elongations at break were almost the same, and the area under the curve were not much different. Compared to PLA samples from FDM, the acrylic sample produced from SLA had much higher elongation at break under the same flexural test. In Fig. 4F, FDM was tested under the flexural force which was vertical to the deposition layer. The vertical flexural strengths were very low, and higher temperatures could reduce the flexural strength of the FDM samples. In Fig. 4G, the flexural tests from PEX with different extruded temperatures were obtained. Apparently, Lower strengths were obtained when higher extruded temperatures were used. The same results were also shown in the samples produced by PIN in Fig. 4H. Higher processing temperature could degrade PLA samples from every technique which resulted in a lower elongation and strength. PM and PEX provided higher flexural strengths and elongations at break compared to FDM which could be concluded that PM and PEX were better in term of strength and toughness. According to Shore D hardness measurements in Fig. 4I, the hardness results did not provide a predictable trend over different temperature which were around 76–86. The average hardness of the PEX samples were among the highest and the average hardness of PM samples were among the lowest. The XRD of polymer from different fabrication techniques were shown in Fig. 4J. The PEX samples had the least crystallinity and PM with 190 °C showed highest crystallinity. Nevertheless, all polymer structures were amorphous with only partial crystallinity. Amorphous structures were prone to the thermal degradation which was the main reason for the reduction of tensile and flexural strength at elevated processing temperature [31].

3.2. Pixel molding with different materials

The pixel mold from PM could also be used for the fabrication of many materials. In this work, the pixel mold was also used to

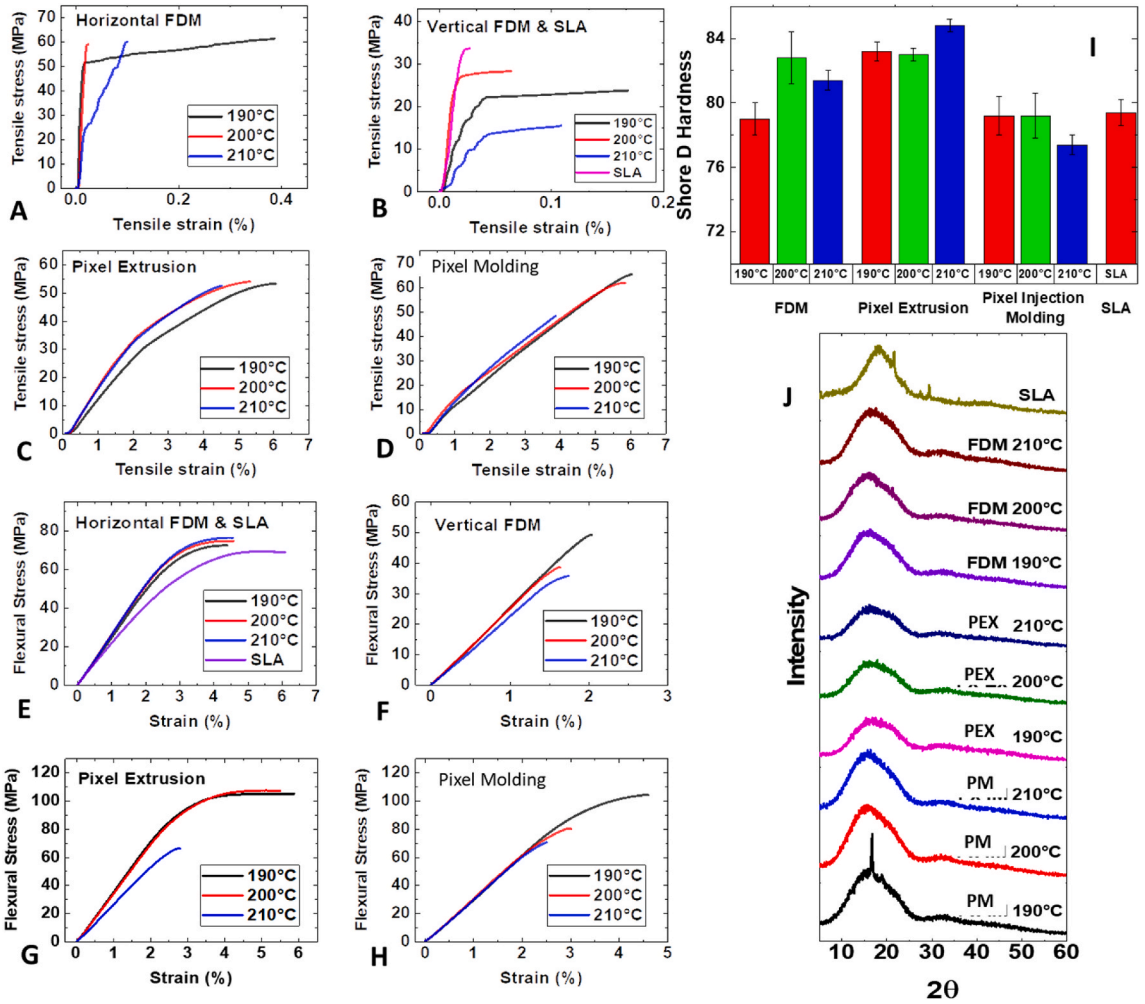

Fig. 4. Tensile test of (A) SLA (B) FDM (C) PEX (D) PM. Flexural test of (E) SLA (F) FDM (G) PEX (H) PM (I) Shore D hardness test of SLA, FDM, PEX and PM and (J) XRD of SLA, FDM, PEX and PM.

fabricate cement, iron (Fe), and silica (SiO_2) as shown in Fig. 5A, B, and 5C respectively. The original size of the mold was 40 × 40 × 65 mm. Cement was casted into the mold by mixing cement powder with water and pour inside the mold. For Fe sample, the 270g of Fe powder was mixed with 30g PMMA which bound Fe powder together. The composite was casted into the mold afterward. After the Fe composite was solidified, the sample was sintered at 500 °C for 3 Hours to eliminate the PMMA binder. The sample was heated at 1100 °C for 5 Hours to sinter Fe powder together. For SiO_2 sample, the 100g silica powder was mixed with 43g PMMA powder and casted into the mold. The sample was heated at 500 °C for 3 Hours to eliminate PMMA and at 550 °C for 5 Hours to sinter SiO_2. The maximum compositions in which composite could still flow and be pressed into the mold was 90% by weight of Fe powder in PMMA and 70% by weight of SiO_2 powder in PMMA. The dimension after casting process was shown in Fig. 5D. Among 3 samples, SiO_2 had highest shrinkage because the filling ratio was only 70%. Once PMMA was burned away, the gaps between SiO_2 powder were decreased and the sample shrank. In Fig. 5E, SEM image depicted the surface morphology of cement sample which composed of large and small porosities. The surface of cement was rough due to the nature of cement solidification process which involved the dehydration of water. In Fig. 5F, the Fe powder with the average particle size of 50 μm was agglomerated. Once mixed with PMMA, the polymer bound Fe particles together as shown in Fig. 4G. The polymer was not thoroughly distributed. Some particles were not covered by PMMA because the amount of PMMA binder was only 10%; however, this Fe/PMMA ratio was sufficient to combine Fe powder together and flow into the mold when pressed. When the green sample of Fe/PMMA composite was sintered at 1100 °C, the particles were well merged with small amount of micro porous in the Fe matrix as shown in Fig. 5H. In Fig. 5I, the average particle size of SiO_2 was 30 μm. In order to inject SiO_2 into the adjustable mold, a higher amount of PMMA needed to be added. The ratio of 30% PMMA in SiO_2/PMMA composite was enough to cover most of the SiO_2 power in the composite as shown in Fig. 5J. The composite was casted inside the adjustable mold and sintered at 550 °C. The powder was merged together with a homogeneous distribution of micro porous as shown in Fig. 5K. In Fig. 5L, the hardness of Fe was highest among three samples. The tensile tests of concrete, Fe, and SiO_2 were shown in Fig. 5M–O. Concrete and SiO_2 which were ceramics had very low elongations at break which were 0.9%. The strength of SiO_2 was twice

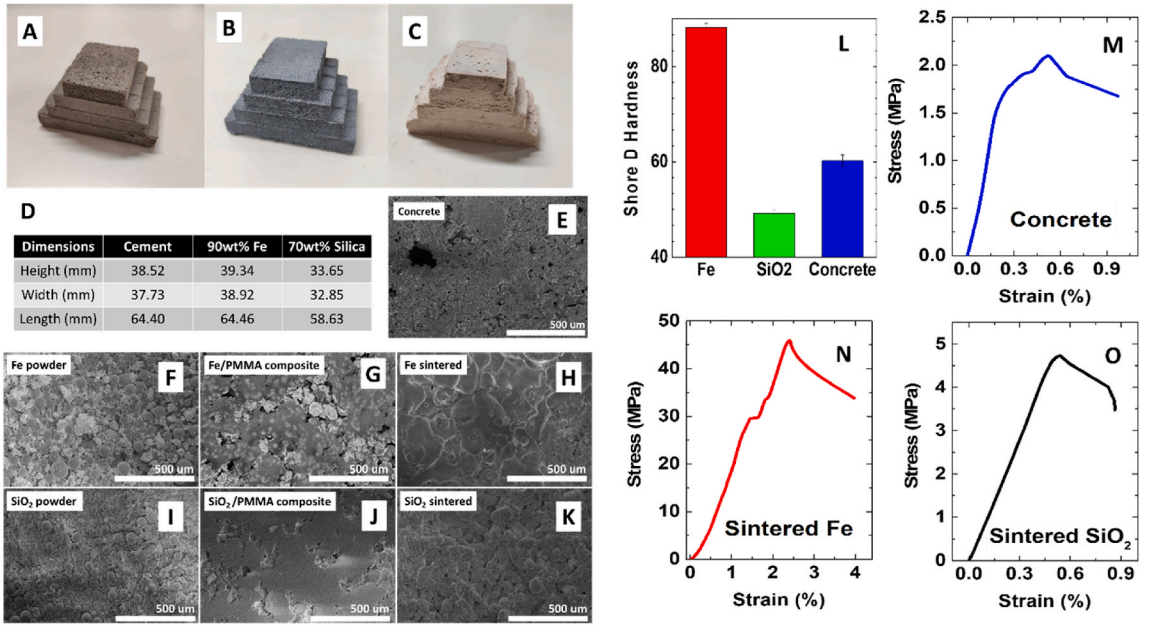

Fig. 5. Pyramid samples fabricated from (A) Cement (B) Fe (C) SiO_2 (D) Dimensions of pyramid samples after PM fabrication. Surface Morphology observe by SEM (E) Cement (F) Fe powder as raw material (G) Fe/PMMA composite after injected into the mold (H) Fe after sintering process (I) SiO_2 powder (J) SiO_2/PMMA composite after injected into the mold (K) SiO_2 after sintering process (L) Shore D hardness of Fe, SiO_2, and Concrete. Tensile test of (M) Concrete (N) Fe and (O) SiO_2.

higher than concrete. The tensile strength of Fe was 45 MPa and elongation at break was 4%. The strength of Fe was much higher than 10 times the strength of SiO_2. The result from hardness test and tensile test depicted that Fe sample was strongest material for PM technique. This work confirmed the possibility to use PM for polymer, polymer composite, metal and ceramics fabrication, and the shape of the sample can be modified accordingly. The resolution of pixel could be improved by reduce the size of each pixel and increase the number of pixels. If the resolution is much better, PIN technique could be another technique for material fabrication for both industrial scale and rapid prototyping scale.

4. Conclusion

PEX and PM were proved to be able to fabricate the rapid 3D modifiable model. The resolution of these techniques were still very rough but they could be improved by reducing size of the hole in PEX and the pin in PM. Although the shape resolutions were not delicate, the microstructure surfaces were smoother compared to the surfaces of the samples from 3D printing. The mechanical properties of PEX and PM such as tensile test, flexural test, including hardness were superior compared to 3D printing. PM technique could also be used to fabricate the ceramics and metal such as cement, silica, and iron which were shown in this work. Obviously, iron which was produced by PM provided the highest mechanical properties. When the size of the pixel is minimized in the future, the resolution of these technique will increased. The fabrication speed which is comparable to the mass production but the shape is adjustable will promote these techniques to be a main production processes in the future.

Conflict of interest

The authors declare no conflict of interest.

Data availability

The raw/processed data in this study are available from the authors upon request.

Acknowledgement

We would like to acknowledge the funding from National Research Council of Thailand N42A650342, and Central Instrument Facility (CIF), Faculty of Science, Mahidol University.

References

[1] J. Junpha, A. Wisitsoraat, R. Prathumwan, W. Chaengsawang, K. Khomungkhun, K. Subannajui, Electronic tongue and cyclic voltammetric sensors based on carbon nanotube/polylactic composites fabricated by fused deposition modelling 3D printing, Mater. Sci. Eng. C 117 (2020), 111319, https://doi.org/10.1016/J.MSEC.2020.111319.

[2] R. Prathumwan, K. Subannajui, Fabrication of a ceramic/metal (Al2O3/Al) composite by 3D printing as an advanced refractory with enhanced electrical conductivity, RSC Adv. 10 (2020) 32301–32308, https://doi.org/10.1039/D0RA01515F.

[3] A. Awad, F. Fina, A. Goyanes, S. Gaisford, A.W. Basit, 3D printing: principles and pharmaceutical applications of selective laser sintering, Int. J. Pharm. 586 (2020), 119594, https://doi.org/10.1016/J.IJPHARM.2020.119594.

[4] J.Z. Manapat, Q. Chen, P. Ye, R.C. Advincula, 3D printing of polymer nanocomposites via stereolithography, Macromol. Mater. Eng. 302 (2017), 1600553, https://doi.org/10.1002/MAME.201600553.

[5] J. Skowyra, K. Pietrzak, M.A. Alhnan, Fabrication of extended-release patient-tailored prednisolone tablets via fused deposition modelling (FDM) 3D printing, Eur. J. Pharmaceut. Sci. 68 (2015) 11–17, https://doi.org/10.1016/J.EJPS.2014.11.009.

[6] J. Gopinathan, I. Noh, Recent trends in bioinks for 3D printing, Biomater. Res. 22 (2018) 1, https://doi.org/10.1186/S40824-018-0122-1, 2018;22:1–15.

[7] Yang Yang, Xiangjia Li, Xuan Zheng, Zeyu Chen, Qifa Zhou, Yong Chen, et al., 3D-Printed biomimetic super-hydrophobic structure for microdroplet manipulation and oil/water separation, Adv. Mater. 30 (2018), 1704912, https://doi.org/10.1002/ADMA.201704912.

[8] C.M. Madla, S.J. Trenfield, A. Goyanes, S. Gaisford, A.W. Basit, 3D printing technologies, implementation and regulation: an overview, AAPS Adv. Pharm. Sci. Ser. 31 (2018) 21–40, https://doi.org/10.1007/978-3-319-90755-0_2/COVER.

[9] N. Martelli, C. Serrano, H. van den Brink, J. Pineau, P. Prognon, I. Borget, et al., Advantages and disadvantages of 3-dimensional printing in surgery: a systematic review, Surgery 159 (2016) 1485–1500, https://doi.org/10.1016/J.SURG.2015.12.017.

[10] X. Chen, W. Liu, B. Dong, J. Lee, H.O.T. Ware, H.F. Zhang, et al., High-speed 3D printing of millimeter-size customized aspheric imaging lenses with sub 7 nm surface roughness, Adv. Mater. 30 (2018), 1705683, https://doi.org/10.1002/ADMA.201705683.

[11] K.J. Leblanc, S.R. Niemi, A.I. Bennett, K.L. Harris, K.D. Schulze, W.G. Sawyer, et al., Stability of high speed 3D printing in liquid-like solids, ACS Biomater. Sci. Eng. 2 (2016) 1796, https://doi.org/10.1021/ACSBIOMATERIALS.6B00184/ASSET/IMAGES/LARGE/AB-2016-00184F_0004, 9 (JPEG).

[12] R. Nazari, R. Nazari, S. Zaare, R.C. Alvarez, R.C. Alvarez, K. Karpos, et al., 3D printing of gas-dynamic virtual nozzles and optical characterization of high-speed microjets, Opt Express 28 (Issue 15) (2020) 21749–21765, https://doi.org/10.1364/OE.390131, 28:21749–65.

[13] D. Perevoznik, D. Perevoznik, R. Nazir, R. Nazir, R. Kiyan, R. Kiyan, et al., High-speed two-photon polymerization 3D printing with a microchip laser at its fundamental wavelength, Opt Express 27 (Issue 18) (2019) 25119–25125, https://doi.org/10.1364/OE.27.025119, 27:25119–25.

[14] P. Wang, B. Zou, S. Ding, L. Li, C. Huang, Effects of FDM-3D printing parameters on mechanical properties and microstructure of CF/PEEK and GF/PEEK, Chin. J. Aeronaut. 34 (2021) 236–246, https://doi.org/10.1016/J.CJA.2020.05.040.

[15] Q. Ge, Z. Li, Z. Wang, K. Kowsari, W. Zhang, X. He, et al., Projection micro stereolithography based 3D printing and its applications, Int. J. Extrem. Manuf. 2 (2020), 022004, https://doi.org/10.1088/2631-7990/AB8D9A.

[16] M. Mukhtarkhanov, A. Perveen, D. Talamona, Application of stereolithography based 3D printing technology in investment casting, Micromachines 11 (2020) 946, https://doi.org/10.3390/MI11100946, 2020;11:946.

[17] A. Kelkar, R. Nagi, B. Koc, Geometric algorithms for rapidly reconfigurable mold manufacturing of free-form objects, Comput. Aided Des. 37 (2005) 1–16, https://doi.org/10.1016/J.CAD.2004.03.001.

[18] B. Koc, S. Thangaswamy, Design and analysis of a reconfigurable discrete pin tooling system for molding of three-dimensional free-form objects, Robot. Comput. Integrated Manuf. 27 (2011) 335–348, https://doi.org/10.1016/J.RCIM.2010.07.017.

[19] H. Quan, T. Zhang, H. Xu, S. Luo, J. Nie, X. Zhu, Photo-curing 3D printing technique and its challenges, Bioact. Mater. 5 (2020) 110–115, https://doi.org/10.1016/J.BIOACTMAT.2019.12.003.

[20] Y. Tian, C.X. Chen, X. Xu, J. Wang, X. Hou, K. Li, et al., A review of 3D printing in dentistry: technologies, affecting factors, and applications, Scanning (2021) 2021, https://doi.org/10.1155/2021/9950131.

[21] N. Vaidya, O. Solgaard, 3D printed optics with nanometer scale surface roughness, Microsys. Nanoengin. (2018 4) 1, https://doi.org/10.1038/s41378-018-0015-4, 2018;4:1–8.

[22] J. Cho, J.H. Park, J.K. Kim, E.F. Schubert, White light-emitting diodes: history, progress, and future, Laser Photon. Rev. 11 (2017), 1600147, https://doi.org/10.1002/LPOR.201600147.

[23] K.D. Jandt, R.W. Mills, A brief history of LED photopolymerization, Dent. Mater. 29 (2013) 605–617, https://doi.org/10.1016/J.DENTAL.2013.02.003.

[24] D. Annicchiarico, J.R. Alcock, Review of factors that affect shrinkage of molded part in injection molding, 29:662–82, https://doi.org/10.1080/10426914.2014.880467, 2014.

[25] V.A. Beloshenko, Y.E. Beygelzimer, V.N. Varyukhin, Thermal shrinkage of polymer mixtures obtained by solid-state extrusion, Polymer 41 (2000) 3837–3840, https://doi.org/10.1016/S0032-3861(99)00553-4.

[26] U.M. Dilberoglu, S. Simsek, U. Yaman, Shrinkage Compensation Approach Proposed for ABS Material in FDM Process, vol. 34, 2019, p. 993, https://doi.org/10.1080/10426914.2019.1594252, 8.

[27] V. Durga Prasada Rao, P. Rajiv, V. Navya Geethika, Effect of fused deposition modelling (FDM) process parameters on tensile strength of carbon fibre PLA, Mater. Today Proc. 18 (2019) 2012, https://doi.org/10.1016/J.MATPR.2019.06.009. –8.

[28] D. Syrlybayev, B. Zharylkassyn, A. Seisekulova, M. Akhmetov, A. Perveen, D. Talamona, Optimisation of strength properties of FDM printed parts—a critical review, Polymers 13 (2021) 1587, https://doi.org/10.3390/POLYM13101587, 2021;13:1587.

[29] LP de Melo, G.V. Salmoria, E.A. Fancello, C.R.D.M. Roesler, Effect of injection molding melt temperatures on PLGA craniofacial plate properties during in vitro degradation, Int. J. Biomater. 2017 (2017), https://doi.org/10.1155/2017/1256537.

[30] I. Rex, B.A. Graham, M.R. Thompson, Studying single-pass degradation of a high-density polyethylene in an injection molding process, Polym. Degrad. Stabil. 90 (2005) 136–146, https://doi.org/10.1016/J.POLYMDEGRADSTAB.2005.03.002.

[31] K. Pal, V. Panwar, S. Friedrich, M. Gehde, An Investigation on Vibration Welding of Amorphous and Semicrystalline Polymers, vol. 31, 2015, p. 372, https://doi.org/10.1080/10426914.2015.1019111, 8.

[32] Kuang Xiao, Zeang Zhao, Kaijuan Chen, Daining Fang, Guozheng Kang, H. Jerry Qi, et al., High-speed 3D printing of high-performance thermosetting polymers via two-stage curing, Macromol. Rapid Commun. 39 (2018), 1700809, https://doi.org/10.1002/MARC.201700809.